Tetrameric assembly of KvLm K^+ channels with defined numbers of voltage sensors

Ruhma Syeda[a,b], Jose S. Santos[b], Mauricio Montal[b,1], and Hagan Bayley[a,1]

[a]Department of Chemistry, University of Oxford, Mansfield Road, Oxford OX1 3TA, United Kingdom; and [b]Section of Neurobiology, Division of Biological Sciences, University of California, San Diego, La Jolla, CA 92093

Edited by Ehud Y. Isacoff, U.C. Berkeley, Berkeley, CA, and accepted by the Editorial Board August 31, 2012 (received for review April 3, 2012)

Voltage-gated K^+ (Kv) channels are tetrameric assemblies in which each modular subunit consists of a voltage sensor and a pore domain. KvLm, the voltage-gated K^+ channel from *Listeria monocytogenes*, differs from other Kv channels in that its voltage sensor contains only three out of the eight charged residues previously implicated in voltage gating. Here, we ask how many sensors are required to produce a functional Kv channel by investigating heterotetramers comprising combinations of full-length KvLm (FL) and its sensorless pore module. KvLm heterotetramers were produced by cell-free expression, purified by electrophoresis, and shown to yield functional channels after reconstitution in droplet interface bilayers. We studied the properties of KvLm channels with zero, one, two, three, and four voltage sensors. Three sensors suffice to promote channel opening with FL_4-like voltage dependence at depolarizing potentials, but all four sensors are required to keep the channel closed during membrane hyperpolarization.

lipid bilayers | membrane proteins | voltage gated potassium channels | membrane reconstitution

Depolarization activated, voltage-gated K^+-selective channels (Kv) comprise four identical subunits each contributing a complete voltage sensor (S1–S4) and a quarter of the ion-conductive pore (S5–S6) (1, 2) (Fig. 1*A*). Upon membrane depolarization, the positively charged transmembrane segment S4 in each voltage sensor moves outward from its resting state and induces conformational changes in the pore. Between the resting and the open state, the channel undergoes a number of kinetic transitions. Transitions between the resting state and the last step that precedes opening and outward K^+ flux define the voltage-dependent "activation" of the channel. In the Kv *Shaker*, activation entails at least five kinetic transitions observable as gating currents: Three early transitions that are voltage-dependent but noncooperative are followed by two late transitions (3–5). At the end of the activation pathway, each subunit is in an "activated-not-open" conformation (6, 7) referring to the state of the sensor and pore, respectively. Although it is well established that each sensor moves independently during the early transitions in activation (8), the nature of the interactions between subunits in Kv channels underlying the transition from activated-not-open to open (the opening transition) remains unsettled (6, 9–12). Structurally, the late kinetic transitions are considered to arise from conformational changes in the S4–S5 linker (7, 13), whereas the final opening transition (6, 7) entails a change in conformation of S6, which forms the bundle-crossing of the pore (activation gate).

To determine the interplay between subunits underpinning the voltage dependence of the opening transition, it is necessary to uncouple it from the activation transitions that precede it and occur at similar rates. This dissection is possible when the opening transition is delayed or blocked. In *Shaker*, this has been achieved by blocking with 4-aminopyridine (7, 14, 15) or by mutations, including a single mutation at the beginning of the linker between the sensor and the pore (L382V) (3) or a triple mutation (ILT) in the S4 segment of the sensor (6, 10, 16, 17). Alternatively, the assembly of hetero-oligomers composed of wild-type (WT) and mutant Kv subunits was explored as a means to examine inter-subunit interactions during voltage-dependent activation (4, 6, 9–12, 16–25). In these studies, hetero-oligomers were assembled either by coexpression of mutant and WT subunits or by fixing the stoichiometry and arrangement of WT and mutant subunits in the oligomer through fusion of the genes encoding them in the desired order. Collectively, the inferences derived from findings with *Shaker* agree that the opening step is weakly voltage-dependent or voltage-independent (10, 21, 22), yet they differ on the degree of cooperativity underlying the transition (6, 11, 12).

To explore the role of voltage sensors in the activation and opening of KvLm, we exploited the structural independence of the pore and sensor modules (26–30), together with the weak voltage-dependent gating of the sensorless pore module (PM) (S4–S5 linker–S5–S6) relative to the full-length channel (FL) (S1–S6) (31–33), to produce functional heterotetramers (Fig. 1*B*). To accomplish this goal, we extended a method used in our laboratory (34–36) and by others (37) to produce mixtures of heteromers by in vitro transcription and translation (IVTT), followed by the separation of defined heteromers by gel electrophoresis (Fig. 1*C*). By this means, channels containing from zero to four voltage sensors were generated. Droplet interface lipid bilayers (DIBs) (38, 39), formed between two lipid monolayer-encased aqueous nanoliter droplets submerged in hexadecane, were used to measure the single-channel conduction and gating properties of the heteromers. This strategy allowed us to show that (*i*) at least three sensors are required to open a channel upon depolarization that displays single-channel conductance, open-state occupancy (P_o), and burst duration values similar to those of the homotetramer comprising full-length subunits; (*ii*) three or four sensors dramatically increase the P_o relative to channels with zero, one, or two sensors by converting a large number of openings to long bursts; (*iii*) the opening frequency after a long closure is largely insensitive to the number of sensors present; (*iv*) all four sensors are needed to completely close the channel upon hyperpolarization; and (*v*) the current–voltage (I–V) properties of the open channel are largely unmodified whether sensor modules are present or not.

Results

Functional Equivalence of KvLm-FL and KvLm-PM Proteins Produced by IVTT or Bacterial Expression. Because correct oligomerization may not reflect native folding and therefore normal function, single-channel currents from FL and PM homotetramers (FL_4

Author contributions: R.S., J.S.S., M.M., and H.B. designed research; R.S. and J.S.S. performed research; R.S., J.S.S., and M.M. analyzed data; and R.S., J.S.S., M.M., and H.B. wrote the paper.

The authors declare no conflict of interest.

This article is a PNAS Direct Submission. E.Y.I. is a guest editor invited by the Editorial Board.

Freely available online through the PNAS open access option.

[1]To whom correspondence may be addressed. E-mail: hagan.bayley@chem.ox.ac.uk or mmontal@ucsd.edu.

This article contains supporting information online at www.pnas.org/lookup/suppl/doi:10.1073/pnas.1205592109/-/DCSupplemental.

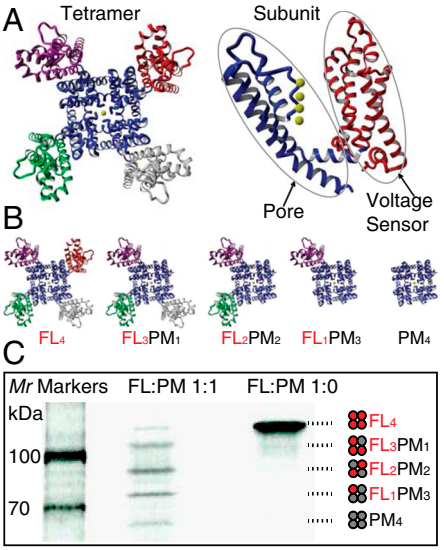

Fig. 1. Modularity of Kv channels. (*A*) Structural modularity of Kv channels. (*Left*) The crystal structure of the Kv1.2-Kv2.1 chimeric channel (Protein Data Bank ID code 2R9R) (28), a member of the *Shaker* family of eukaryotic Kv channels, showing the four well separated voltage-sensor modules, S1–S4 (red, magenta, green, and gray), surrounding a pore module (blue). (*Right*) A single subunit of the Kv1.2-Kv2.1 chimera with the sensor and pore depicted in red and blue. The yellow spheres represent K^+ ions. All structures were rendered using YASARA (http://www.yasara.org). (*B*) Representations of tetrameric assemblies with different numbers of voltage sensors (from left to right: four, three, two, one, and zero). (*C*) Assembly modularity of KvLm: heterotetramers assembled by coexpressing FL and PM polypeptides in a cell-free expression system. The tetramers were separated in a 7.5% Tris-HCl SDS polyacrylamide gel. The polypeptides were labeled with L-[^{35}S]methionine and visualized by autoradiography. KvLm DNA ratios in the expression system were (FL:PM): 1:1 and 1:0. Empty lanes were left between samples to avoid cross-contamination when extracting tetrameric protein assemblies from the gel. The cartoons illustrate the combinations of subunits in the tetramers. Note that FL_2PM_2 can adopt two possible configurations (i.e., FL subunits adjacent to each other or diagonally opposed); only one is depicted here for clarity.

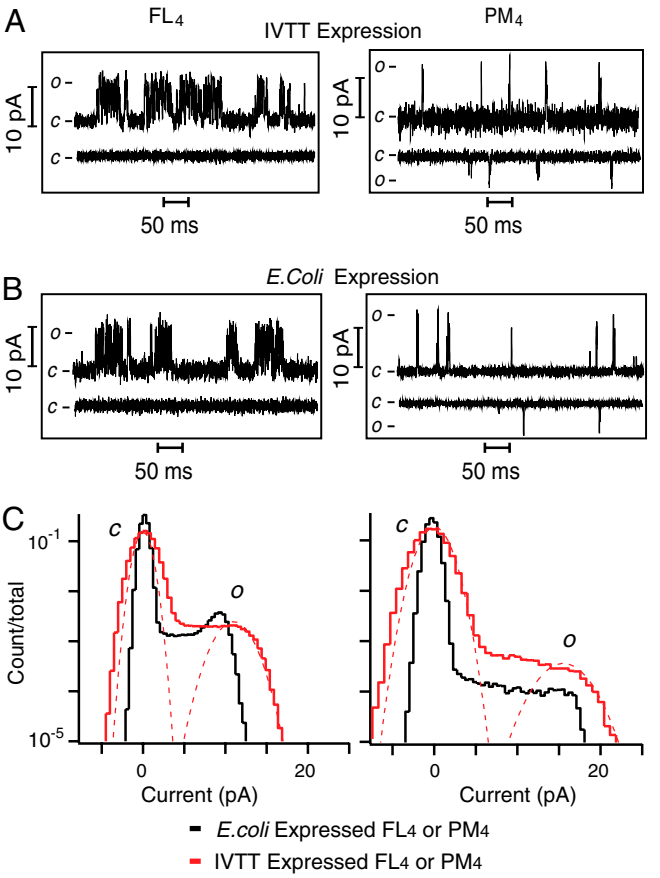

Fig. 2. Single-channel currents of KvLm recorded in DIBs. (*A*) Single-channel currents of KvLm FL_4 and PM_4 homotetramers produced by IVTT expression or (*B*) by *E. coli* expression, after reconstitution in DIBs. Single-channel currents were recorded at $V = +150$ mV and $V = -150$ mV. *c* and *o* denote closed and open. (*C*) Single-channel all-points current histograms of FL_4 (*Left*) and PM_4 (*Right*) expressed either by IVTT (red) or in *E. coli* (black). Currents were recorded at $V = +150$ mV. γ of FL_4 expressed by IVTT $= 73 \pm 7$ pS, and that of $PM_4 = 113 \pm 7$ pS. γ of FL_4 expressed in *E.coli* $= 66 \pm 7$ pS, and that of $PM_4 = 105 \pm 10$ pS.

and PM_4) produced by expression in *Escherichia coli* (Fig. 2*B*) (31) were compared to those expressed by IVTT (Fig. 2*A*). The single-channel conductance (γ) of FL_4 expressed by IVTT was 73 ± 7 pS (determined by a Gaussian fit to the open state in a current histogram; Fig. 2*C*), whereas that of PM_4 was 113 ± 7 pS, at $V = +150$ mV in 0.5 M KCl, 10 mM HEPES, pH 7.4 ($n = 4$). Under identical conditions, γ of FL_4 expressed in *E. coli* was 66 ± 7 pS, while that of PM_4 was 105 ± 10 pS ($n = 4$) (Fig. 2*C*). The steady-state P_o of FL_4 and PM_4 homotetramers produced by IVTT or by expression in *E. coli* were also compared. At a depolarizing potential (+150 mV), the P_o of FL_4 expressed by IVTT was $4.0 \pm 0.4 \times 10^{-2}$ and that of PM_4 was $1.0 \pm 0.5 \times 10^{-3}$ (Table 1); the corresponding values for FL_4 and PM_4 expressed in *E. coli* were $3.7 \pm 0.7 \times 10^{-2}$ and $1.3 \pm 0.8 \times 10^{-3}$. At a hyperpolarizing potential (−150 mV), FL_4 channels expressed either by IVTT (Fig. 2*A*) or in *E. coli* (Fig. 2*B*) failed to open, a hallmark of Kv channels; by contrast, P_o for PM_4 expressed by IVTT was $6 \pm 1 \times 10^{-4}$ and in *E. coli* was $4 \pm 2 \times 10^{-4}$. The near equivalence of γ together with the similar patterns of activity at positive and negative potentials demonstrates that the two methods of protein expression produce channels with similar functional properties. This implies that both FL_4 and PM_4 proteins retain a native fold and function even after separation by SDS gel electrophoresis (Fig. 1*C*).

Coexpression of KvLm-FL and KvLm-PM Subunits Yields Heterotetramers that Are SDS Resistant. Coexpression of KvLm-FL and KvLm-PM proteins by coupled IVTT generated SDS-resistant hetero-oligomers that were separated according to their size by electrophoresis in a 7.5% SDS polyacrylamide gel (Fig. 1*C*). Five bands were observed, with apparent molecular weights (M_r) of 68, 80, 95, 105, and 115 kDa. These values are in good agreement with the calculated masses of tetramers for all possible subunit stoichiometries: PM_4(73 kDa), FL_1PM_3 (84 kDa), FL_2PM_2 (96 kDa), FL_3PM_1 (107 kDa), and FL_4 (119 kDa). Proteins were extracted from fractions excised as bands from the gels (see *Materials and Methods*) and all single-channel recordings were performed by reconstituting distinct tetrameric assemblies in DIBs.

Single-Channel Conductance Properties of Heteromers. Representative steady-state single-channel currents recorded at $V = +150$ mV and $V = -150$ mV (Fig. 3) show that all KvLm heteromers produced by cell-free expression (Fig. 1*C*) yield functional channels after reconstitution in lipid bilayers. To discern the differences in permeation and gating of each heteromer, segments of the records are displayed at higher time resolution in the corresponding right panels (Fig. 3). Only single-channel records were selected for analysis; those displaying two or more concurrent channel openings were excluded. The homotetramers FL_4 and PM_4 exhibit the single-channel properties previously characterized by Santos et al. (31): FL_4 exhibits clusters of channel openings (bursts) (Fig. 3*A*) with intraburst closures $\lesssim$15 ms (τ_{crit}; see *Materials and Methods*), which are terminated by interburst closures $\gtrsim$15 ms, whereas PM_4 (Fig. 3*E*) displays primarily isolated, short openings. In both cases,

Table 1. Single-channel characteristics of KvLm homotetramers and heterotetramers

Tetramer	Conductance, pS	Open-state lifetime, ms*	Open-state occupancy	Closed-state occupancy	Median burst duration, ms	Bursts per second
FL_4	73 ± 7	1.9 ± 0.3	$4.0 \pm 0.4 \times 10^{-2}$	0.9 ± 0.1	16 ± 3	5 ± 1
FL_3PM_1	93 ± 7	1.7 ± 0.3	$5.0 \pm 0.5 \times 10^{-2}$	0.7 ± 0.1	11 ± 3	13 ± 2
FL_2PM_2	73 ± 2	0.3 ± 0.2†	$2 \pm 2 \times 10^{-4}$	<< 0.1†	NA	NA
FL_1PM_3	93 ± 7	1.5 ± 0.3	$2 \pm 1 \times 10^{-3}$	0.9 ± 0.1	5 ± 0.4	0.4 ± 0.3
PM_4	113 ± 7	1.4 ± 0.3	$1.0 \pm 0.5 \times 10^{-3}$	0.9 ± 0.1	4 ± 0.2	0.7 ± 0.3

Single-channel properties recorded at V = +150 mV for homotetrameric and heterotetrameric assemblies composed of KvLm-FL and KvLm-PM subunits.
*It is worth noting that fittings of open time distributions of all assemblies but FL_4 miss a short-lived component (<1 ms) (Figs. S2 and S3). The conjecture that all four sensors stabilize the open state is in line with these observations notwithstanding the limitation of our recording system to resolve such brief openings.
†For FL_2PM_2, open- and closed-state lifetimes are estimates given that the time resolution of the recording prevents rigorous determinations. Open and closed state occupancies do not add up to 1 because the channel resides in a subconductance state(s) for a fraction of the time.

the single-channel current fluctuates between open and closed states, including the occurrence of at least two subconductance states (substates denoted as S) (Fig. S1). Notably, these substates are predominantly visited during the closing of the channel, similarly to what is seen in *Shaker* (40); by contrast, channel opening remains an all-or-none process independent of the number of sensors present (except for constructs with two sensors; see below). To focus on the fully open state of the channel (i.e., when all subunits are in the conducting conformation) without contamination from residency in substates (40–42), we separated the open states by event detection with the segmental *k*-means algorithm (SKM) implemented in QuB (see *Materials and Methods*). Here, we focus only on the open-state amplitude, lifetime, P_o, and bursting frequency at $V = +150$ mV, a potential at which the P_o for each construct is nearly saturated (see below). At +150 mV, the γ values are: $FL_4 = 73 \pm 7$ pS, $FL_3PM_1 = 93 \pm 7$ pS, $FL_2PM_2 = 73 \pm 2$ pS, $FL_1PM_3 = 93 \pm 7$ pS, and $PM_4 = 113 \pm 7$ pS. These values indicate that γ for FL_4 is the smallest (except for FL_2PM_2) and that the inclusion of one or more PM subunit increases γ by more than 20%. Inspection of the single-channel currents for FL_2PM_2 shows that, unlike the other tetramers, it exhibits extremely brief openings. At first sight, these fluctuations appear erratic and irregular; however, they are indeed features of the FL_2PM_2 heteromer given that they can be entirely eliminated by exposure to 100 μM tetrabutylammonium (TBA), a Kv channel blocker that blocks both PM_4 and FL_4 (31). It is noteworthy that the FL_2PM_2 heteromer rarely resides in the open or closed state: It dwells most of the time in a low-amplitude substate (Fig. 3*C*). We conjecture that the low value of γ measured for FL_2PM_2 arises either from the failure of the construct to open to full conduction or because the openings are too short for the amplitude to be correctly determined by the recording system.

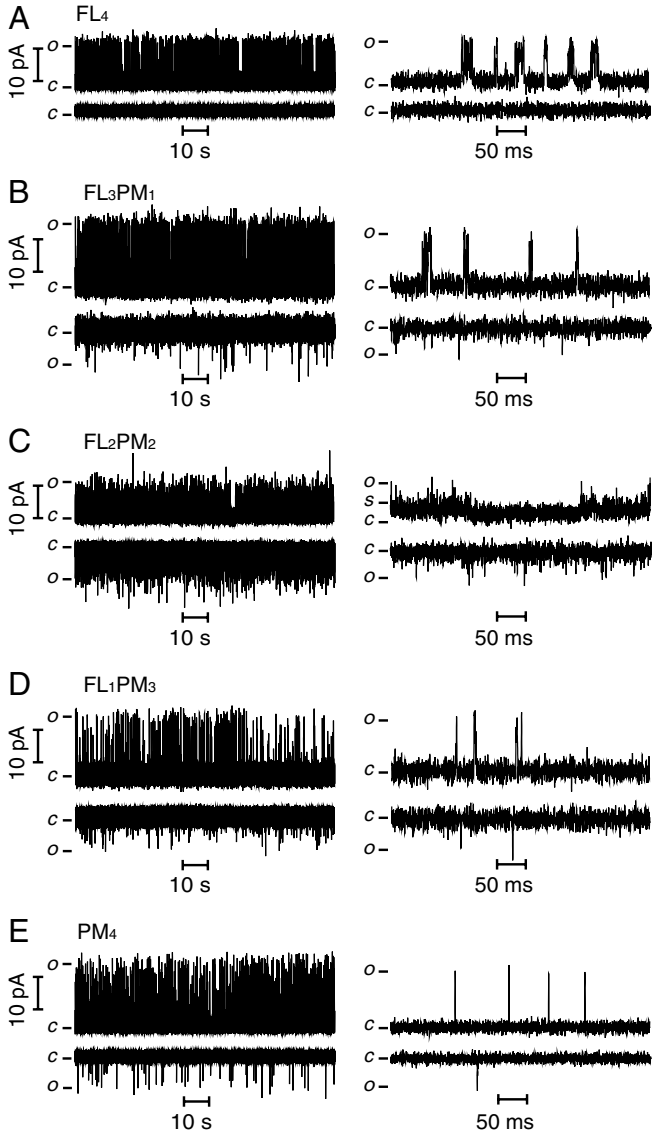

Fig. 3. Single-channel activity of heteromeric KvLm channels recorded in DIBs. (*A*) FL_4. (*B*) FL_3PM_1. (*C*) FL_2PM_2. (*D*) FL_1PM_3. (*E*) PM_4. Single-channel currents of KvLm tetramers were recorded at $V = +150$ mV (*Upper*) and $V = -150$ mV (*Lower*). Segments of the same recordings are shown on an expanded time scale (*Right*).

All Four Voltage Sensors Are Required for Rectification. All heteromers containing PM subunits display single-channel currents under both depolarizing and hyperpolarizing conditions. By contrast, no current was detected for FL_4 at negative applied voltages ($P_o << 6 \times 10^{-6}$) (Figs. 3 and 4*A*). The implication is that all four voltage sensors in a tetramer are required to keep the channel fully closed at negative potentials. This is consistent with the proposed principal role of the voltage sensor in Kv channels: To keep the channel closed at hyperpolarizing membrane potentials (43, 44). In addition, the failure of three FL subunits to coerce a fourth PM subunit to close at hyperpolarizing potentials suggests that channel closing at hyperpolarizing potentials is not cooperative in KvLm.

Only Three Sensors Are Required for Intact Voltage-Dependent Gating and Maximum P_o. To investigate the coupling of the voltage sensor to pore opening, we determined the P_o of each heteromer at potentials ranging from 0 to +200 mV (Fig. 4*B*). Two striking features emerge from the analysis. First, the P_o of channels with three or more sensors saturates at values approximately 20-fold larger than for those channels with zero or one sensor. Second, a two-state Boltzmann fit to the data shows that the slope of the fitting function ("*z*", the apparent gating charge) increases approximately 3-fold upon acquisition of three or more sensors (Fig. 4*C*).

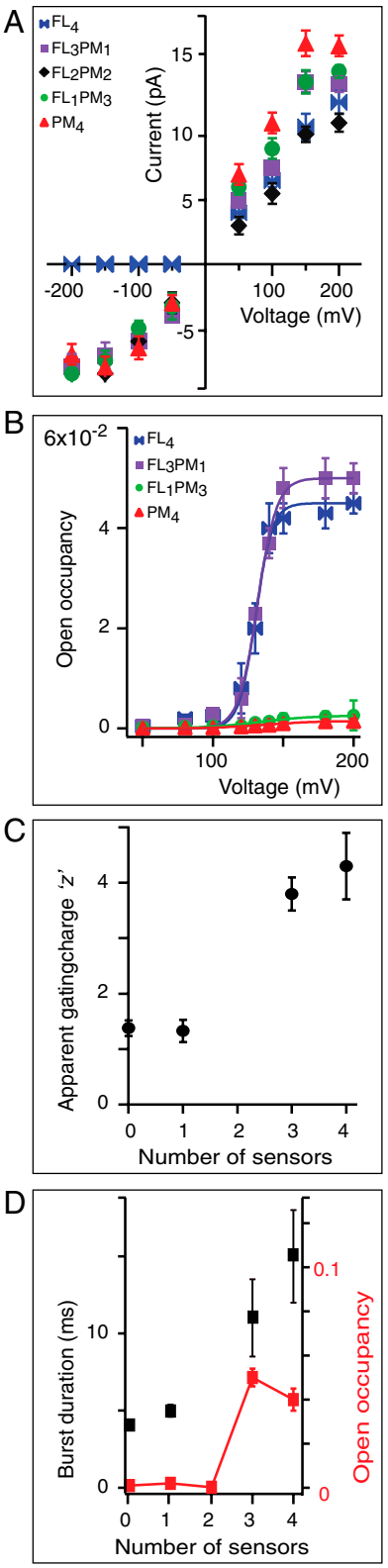

Fig. 4. Permeation and gating properties of KvLm tetramers. (*A*) I–V curves of KvLm homotetramers and heterotetramers. FL_4 did not open at negative potentials. (*B*) Open occupancy (P_o) curves for homotetramers and heterotetramers. The smooth curves represent the best fit of the Boltzmann function to the data. (*C*) Increase in apparent gating charge with the number of voltage sensors in a tetramer. (*D*) P_o (red squares) and median burst duration (black squares) as functions of the number of voltage sensors in the assembly. $V = +150$ mV. Error bars represent SEM; the number of experiments for each tetrameric assembly was ≥4.

Channel Closing at Activating Potentials Is Determined by the Sensor. The heightened P_o in channels with three or four sensors at saturating potentials may result from an increase in the frequency of opening, an increase in the bursting frequency, an increase in mean open time, or an increase in burst duration. To identify the culprit(s), we analyzed the distribution of closed and open dwell times and determined the median burst duration and burst frequency at +150 mV for each oligomeric assembly (Figs. S2 and S3 and Table 1). Focusing first on the role of the sensor in closing the channel, we find that the open dwell times of all tetramers are fit by a single component probability density function with characteristic open dwell lifetimes that appear insensitive to the number of sensors: (PM_4) 1.4 ± 0.3 ms, (FL_1PM_3) 1.5 ± 0.3 ms, (FL_2PM_2) 0.3 ± 0.2 ms, (FL_3PM_1) 1.7 ± 0.3 ms, and (FL_4) 1.9 ± 0.3 ms. In contrast, burst analysis shows that the addition of three or more sensors increases significantly the median burst duration relative to channels with one or no sensors; in this way, the sensor contributes to the stability of the open conductive state (Table 1 and Fig. 4*D*). Furthermore, the roles of the sensors in this process are not independent because three or more sensors are required to evoke the change.

Channel Opening Is Insensitive to the Number of Sensors Present. The closed dwell-time distributions of all heteromers, apart from FL_2PM_2 (Fig. S4), are well fit with two time constants (τ_1 and τ_2) that differ in duration by approximately 100-fold, a property of bursting channels (Figs. S2 and S3). To investigate the role of the sensor in evoking the transition from closed to open, we asked if the frequency with which the channel transits from a long closure ($>\tau_{crit}$) to the open state is a function of the number of sensors. Our analysis (see *Materials and Methods*) shows no correlation: 9 ± 3 s^{-1} for PM_4, 4 ± 3 s^{-1} for FL_1PM_3, 25 ± 3 s^{-1} for FL_3PM_1, and 10 ± 3 s^{-1} for FL_4. This analysis strongly suggests that probability of transiting from a long closure to the open state is insensitive to the number of sensors present. The observation that the burst frequency increases from 0.7 ± 0.3 s^{-1} in PM_4 to 5 ± 1 s^{-1} in FL_4 indicates that while for PM only 0.7 out of 9 openings become bursts, 5 out of 10 openings mark the beginning of a burst for FL_4. This analysis is consistent with the notion that the primary role of the sensor is to convert short openings, as manifested in PM_4, into long bursts in FL_4.

Discussion

In 2008, Santos et al. demonstrated that, in the absence of all sensors, the pore of KvLm retains full selectivity and weak voltage-dependent gating (31). These findings validated an early prediction (45–47) and contemporary structural data (27, 28), which suggested that Kv channels are modular assemblies of four sensor modules and one pore. Here, we have assessed the modularity of Kv channels by assembling tetramers lacking sensor domains. Specifically, we aimed to answer the question: What is the role of the voltage-sensor in opening and closing of KvLm?

Modular Design of Kv Channels. First, we showed that purified heterotetramers of KvLm-FL and KvLm-PM subunits, synthesized by using a cell-free expression system, are active after reconstitution in lipid bilayers. This engineering success demonstrates that, within the KvLm subunit, proper folding of voltage sensor and PMs is largely independent and that correct oligomerization is achieved with any number of sensors. We therefore suggest that the pore-only construct (KvLm-PM, PM_4) might embody a valuable and robust scaffold for the assembly of novel Kv channels by the attachment of designed sensors to each of the four "accepting" pore subunits.

Sensor Contribution to P_o: A Role for the Sensor in Keeping the Channel Open. Second, we showed that the open-state occupancy of KvLm is determined by the gating phenotype of the most abun-

dant subunit in the heteromer. If the oligomer has more FL than PM subunits, the channel gates with the efficacy of FL_4. Conversely, if the assembly has more PM than FL subunits, the channel gates with the low P_o characteristic of the sensorless PM_4. Burst analysis demonstrates that the observed difference in P_o correlates with burst duration as well as with burst frequency: Channels with three or four sensors exhibit burst durations approximately 2- to 4-fold longer and undergo bursting at least 7-fold more frequently than channels with zero or one sensor. The nonlinear increase in burst duration and burst frequency upon incremental addition of FL subunits, and the finding that at least three sensors are required to support an FL_4-like channel suggest that channel opening is sustained by a complex set of interactions between voltage sensors.

Subunit Contribution to Absolute Rectification: A Role for the Sensor in Channel Closing. All four sensors are required for full closure (Figs. 3*A* and 4*A*). This indicates that at hyperpolarizing potentials the structure of the pore in the absence of one or more sensors is different from that in FL_4. The simplest explanation is that in the absence of just one sensor the pore cannot be sealed closed. Presumably, in the KvLm pore, all four sensors must do work against the repulsion between the highly charged C-terminal S6 sequences (RAKK) at the bundle crossing where the "activation" gate closes.

Concluding Remarks

What is the role of each sensor in Kv channels? We speculate that, without the sensor module, the PM resides in a conformation ready to open, presumably in a state between closed-activated and open. Here we show that sensor must do two jobs: Keep the channel closed at hyperpolarizing potentials (Figs. 3*A* and 4*A*) and keep it open at depolarizing potentials (Fig. 4 *B* and *D*). Both of these roles have been proposed for the voltage-sensors in eukaryotic channels (43, 44) suggesting a similar mechanism of operation among all Kvs. Importantly, the PM also contains a voltage sensor of low efficacy that is insufficient to seal the channel closed, yet competent to gate the channel open (albeit with low P_o). These results suggest that the structural element that gates the pore in the absence of the sensor may include part of the gating charge that participates in the last step before the start of conduction in eukaryotic Kvs (10). This inference naturally leads us to ask: Where is this charged component located in the pore?

Materials and Methods

Cell-Free Expression and Purification of KvLm. KvLm-FL and KvLm-PM genes were cloned in between the NdeI and HindIII restriction sites in the pT7-SC1 expression vector (48). KvLm-FL and KvLm-PM were coexpressed in a cell-free coupled IVTT system to form mixtures of heteromeric KvLm tetramers. The IVTT kit contained an *E. coli* T7-S30 extract optimized for circular DNA (Promega no. L1130). The complete amino acid mixture (5 μL, 1 mM) and premix solution (20 μL) were mixed with *L*-[^{35}S]methionine (2 μL, 1,175 Ci mmol^{-1}, 10 mCi mL^{-1} MP Biomedicals), plasmid DNA (FL: 4 μL, 400 ng μL^{-1}, PM: 4 μL, 400 ng μL^{-1}) and T7-S30 extract (15 μL) supplemented with rifampicin (1 μg mL^{-1}), and then incubated at room temperature for 5 h. *n*-Dodecyl-β-D-maltoside (DDM) was then added to a final concentration of 1 mM to solubilize the expressed protein, and the sample was further incubated for 1 h at room temperature. Laemmli sample buffer (2 ×, 100 μL; Bio-Rad Laboratories) was then added and the sample was loaded, without heating, into a 7.5% Tris-HCl SDS polyacrylamide gel. The gel was run for 12 h at 70 V to achieve maximal separation between the oligomers. The gel was vacuum dried without heating onto 3 MM chromatography paper (GE Healthcare) and visualized by exposure to film (BioMax MR-1; Kodak). Each of the homomer and heteromer-containing bands was cut from the gel by using the autoradiogram as a reference. The cut-out pieces were rehydrated in a buffer (300 μL) containing 10 mM 4-(2-hydroxyethyl)-1-piperazineethanesulfonic acid (HEPES), 1 mM DDM, 10 mM KCl, pH 7.5, for 30 min, and the paper backing of the gel removed. The rehydrated gel pieces were crushed with a pestle (Bellco Glass Inc), transferred to a 0.2-μm cellulose acetate microfilter tube (Rainin) and centrifuged at 25,000 × *g* for 10 min. The eluted protein was aliquoted (20 μL) and stored at −80 °C.

***E. coli* Expression and Purification of KvLm.** *E. coli* expression of KvLm-FL and KvLm-PM was carried out as described before (31).

Lipid Vesicle Preparation and Protein Reconstitution into Liposomes. Liposomes were composed of 90% (mol percent) 1,2-diphytanoyl-*sn*-glycero-3 phosphocholine (DPhPC) and 10% of the negatively charged lipid, 1,2-dioleoyl-*sn*-glycero-3-phosphatidic acid (DOPA) (Avanti Polar Lipids). DPhPC and DOPA stock solutions in chloroform (10 mg mL^{-1}) as obtained from Avanti were mixed in the required ratio. The mixture was transferred to a glass vial, and then dried under a stream of nitrogen. The lipids were further dried under vacuum in a desiccator for 2 h. Buffer (0.5 M KCl, 10 mM HEPES, pH 7.4) was added to the dried lipid mixture to give a final lipid concentration of 0.5 mM, followed by thorough vortexing to ensure mixing. The suspension was subjected to five freeze-thaw cycles, extruded (LIPEX™ Extruder, Northern Lipids) nine times, through two 0.1-μm Isopore membrane filters (Filter code:VCTP01300 Millipore), and stored at 4 °C.

For reconstitution, the IVTT-expressed protein was diluted approximately 20-fold in the liposome suspension, whereas the *E. coli* expressed protein was diluted approximately 100-fold. The protein–lipid mix (proteoliposomes) was incubated on ice for 15 min prior to bilayer recording experiments. All the electrical measurements were performed at room temperature in 0.5 M KCl, 10 mM HEPES, pH 7.4. Fresh aliquots of liposomes and protein were used for every experiment.

Single-Channel Recordings Using DIBs. Single-channel currents were recorded from DIBs as described (38). Briefly, a 10 × 10 × 4 mm Perspex chamber was filled with hexadecane (Sigma Aldrich) containing 1% DPhPC. A 0.1-mm-diameter Ag/AgCl wire electrode was attached to each of two micromanipulators (NMN-21, Narishige). Droplets (approximately 200 nL) were placed with a pipette on each of the electrodes, which had been coated with 3% wt/vol low-melt agarose. The electrode carrying the droplet with the proteoliposomes in 0.5 M KCl, 10 mM HEPES, pH 7.4 was connected to the grounded end of the patch clamp head-stage (Axopatch 200B, Axon Instruments). The second electrode, in a droplet containing liposomes in the same buffer, was connected to the working end of the head stage. The droplets-containing chamber, electrodes, and the amplifier head stage were enclosed in a Faraday cage.

The droplets were incubated in hexadecane at room temperature until a monolayer of lipid had formed around them (approximately 5 min). A bilayer spontaneously formed (49) when the two droplets were brought into contact by using the micromanipulators. The capacitance of the lipid bilayer was determined by applying a triangular voltage wave with a function generator (Iso-Tech GFG-8216A) and maintained at approximately 300 to 400 pF by adjusting the area with the micromanipulators. After bilayer formation, voltage was applied continuously to monitor channel activity. At least four independent experiments were performed for each KvLm tetramer assembly.

Single-Channel Acquisition and Analysis. Single-channel currents were sampled at 10 kHz using an Axon 200B patch-clamp amplifier, filtered by using a low pass Bessel filter (80 dB/decade) with a corner frequency of 1 kHz, and then digitized with a DigiData 1320 A/D converter (Axon Instruments). Only single-channel records were used for analysis. The presence of multiple channels in a bilayer was ascertained by the occurrence of concurrent openings of two or more channels in records lasting more than 3 min under the highest imposed potential, typically +200 mV. Given the low open probability of all the tetramers, this approach is not infallible. All preprocessing and analysis of the single-channel records was performed with QuB software (www.qub.buffalo.edu). Prior to analysis, the single-channel currents were further filtered to a final effective (online + offline) frequency of 700–500 Hz. Event detection was performed by time course fitting with the SKM implemented in QuB (50). To avoid the detection of erroneous events, the receiver dead time (t_d) was set at 300 μs for all records. Therefore, transitions shorter than t_d were ignored, transitions longer than t_d were accepted as "events," and subconductance levels were not counted as openings. The effective gating charge z was obtained from a fit of the open occupancy versus potential (in millivolts) with a two-state Boltzmann function: $P_o = P_{max} * [1 + \exp(z * (F/(R * T)) * (V_{1/2} - V))]^{-1}$ with $F = 9.6485 \times 10^4$ C mol^{-1}, $R = 8.3145 \times 10^3$ mV C mol^{-1}K^{-1}, and $T = 298$ K in IGOR (Wavemetrics).

The single-channel characteristics extracted from the time-course fitting are summarized in Table 1. Bursts were defined as a group of three or more opening transitions with intraburst closures shorter than τ-critical (τ_{crit}) and terminated by an interburst closure longer than τ_{crit}. The value of τ_{crit} was calculated from the closed dwell-time histograms in QuB for each record ($2 \le \tau_{crit} \le 15$ ms). To calculate the frequency with which a channel transits from a long closed period (longer than τ_{crit}) to the open state, we repeated

the calculation for burst number but relaxed the burst definition to include any number of events. Accordingly, in this case, a burst or a single opening event each counted as one transition. The analysis reported here is based on the following number of events for each tetramer: $FL_4 = 20,028$; $FL_3PM_1 = 22,264$; $FL_2PM_2 = 21,738$; $FL_1PM_3 = 12,682$; $PM_4 = 12,575$.

ACKNOWLEDGMENTS. The pT7-SC1 vector was a gift from Dr. Stephen Cheley. We thank Syed Asleh Al-Husaini for his encouragement and support. R.S. was supported in part by a Clarendon Scholarship. This work was funded by the Medical Research Council (H.B.) and the National Institutes of Health (GM-49711 to M.M.).

1. MacKinnon R (2004) Potassium channels and the atomic basis of selective ion conduction (Nobel Lecture). *Angew Chem Int Ed Engl* 43:4265–4277.
2. Tombola F, Pathak MM, Isacoff EY (2006) How does voltage open an ion channel? *Annu Rev Cell Dev Biol* 22:23–52.
3. Schoppa NE, Sigworth FJ (1998) Activation of Shaker potassium channels. III. An activation gating model for wild-type and V2 mutant channels. *J Gen Physiol* 111:313–342.
4. Zagotta WN, Hoshi T, Dittman J, Aldrich RW (1994) Shaker potassium channel gating. II: Transitions in the activation pathway. *J Gen Physiol* 103:279–319.
5. Loboda A, Armstrong CM (2001) Resolving the gating charge movement associated with late transitions in K channel activation. *Biophys J* 81:905–916.
6. Pathak M, Kurtz L, Tombola F, Isacoff E (2005) The cooperative voltage sensor motion that gates a potassium channel. *J Gen Physiol* 125:57–69.
7. del Camino D, Kanevsky M, Yellen G (2005) Status of the intracellular gate in the activated-not-open state of shaker K+ channels. *J Gen Physiol* 126:419–428.
8. Catterall WA (2010) Ion channel voltage sensors: Structure, function, and pathophysiology. *Neuron* 67:915–928.
9. Tytgat J, Hess P (1992) Evidence for cooperative interactions in potassium channel gating. *Nature* 359:420–423.
10. Ledwell JL, Aldrich RW (1999) Mutations in the S4 region isolate the final voltage-dependent cooperative step in potassium channel activation. *J Gen Physiol* 113:389–414.
11. Zandany N, Ovadia M, Orr I, Yifrach O (2008) Direct analysis of cooperativity in multisubunit allosteric proteins. *Proc Natl Acad Sci USA* 105:11697–11702.
12. Gagnon DG, Bezanilla F (2009) A single charged voltage sensor is capable of gating the Shaker K+ channel. *J Gen Physiol* 133:467–483.
13. Batulan Z, Haddad GA, Blunck R (2010) An intersubunit interaction between S4–S5 linker and S6 is responsible for the slow off-gating component in Shaker K+ channels. *J Biol Chem* 285:14005–14019.
14. Armstrong CM, Loboda A (2001) A model for 4-aminopyridine action on K channels: Similarities to tetraethylammonium ion action. *Biophys J* 81:895–904.
15. McCormack K, Joiner WJ, Heinemann SH (1994) A characterization of the activating structural rearrangements in voltage-dependent Shaker K+ channels. *Neuron* 12:301–315.
16. Gagnon DG, Bezanilla F (2010) The contribution of individual subunits to the coupling of the voltage sensor to pore openingin Shaker K channels: Effect of ILT mutations in heterotetramers. *J Gen Physiol* 136:555–568.
17. Smith-Maxwell CJ, Ledwell JL, Aldrich RW (1998) Uncharged S4 residues and cooperativity in voltage-dependent potassium channel activation. *J Gen Physiol* 111:421–439.
18. Isacoff EY, Jan YN, Jan LY (1990) Evidence for the formation of heteromultimeric potassium channels in Xenopus oocytes. *Nature* 345:530–534.
19. Ruppersberg JP, et al. (1990) Heteromultimeric channels formed by rat brain potassium-channel proteins. *Nature* 345:535–537.
20. Kerschensteiner D, Stocker M (1999) Heteromeric assembly of Kv2.1 with Kv9.3: Effect on the state dependence of inactivation. *Biophys J* 77:248–257.
21. Hoshi T, Zagotta WN, Aldrich RW (1994) Shaker potassium channel gating. I: Transitions near the open state. *J Gen Physiol* 103:249–278.
22. Schoppa NE, Sigworth FJ (1998) Activation of shaker potassium channels. I. Characterization of voltage-dependent transitions. *J Gen Physiol* 111:271–294.
23. Smith-Maxwell CJ, Ledwell JL, Aldrich RW (1998) Role of the S4 in cooperativity of voltage-dependent potassium channel activation. *J Gen Physiol* 111:399–420.
24. Horn R, Ding S, Gruber HJ (2000) Immobilizing the moving parts of voltage-gated ion channels. *J Gen Physiol* 116:461–476.
25. Bao H, Hakeem A, Henteleff M, Starkus JG, Rayner MD (1999) Voltage-insensitive gating after charge-neutralizing mutations in the S4 segment of Shaker channels. *J Gen Physiol* 113:139–151.
26. Lee SY, Banerjee A, MacKinnon R (2009) Two separate interfaces between the voltage sensor and pore are required for the function of voltage-dependent K(+) channels. *PLoS Biol* 7:e47.
27. Long SB, Campbell EB, Mackinnon R (2005) Crystal structure of a mammalian voltage-dependent Shaker family K+ channel. *Science* 309:897–903.
28. Long SB, Tao X, Campbell EB, MacKinnon R (2007) Atomic structure of a voltage-dependent K+ channel in a lipid membrane-like environment. *Nature* 450:376–382.
29. Chakrapani S, Cuello LG, Cortes DM, Perozo E (2008) Structural dynamics of an isolated voltage-sensor domain in a lipid bilayer. *Structure* 16:398–409.
30. Butterwick JA, MacKinnon R (2010) Solution structure and phospholipid interactions of the isolated voltage-sensor domain from KvAP. *J Mol Biol* 403:591–606.
31. Santos JS, Grigoriev SM, Montal M (2008) Molecular template for a voltage sensor in a novel K+ channel. III. Functional reconstitution of a sensorless pore module from a prokaryotic Kv channel. *J Gen Physiol* 132:651–666.
32. Santos JS, Lundby A, Zazueta C, Montal M (2006) Molecular template for a voltage sensor in a novel K+ channel. I. Identification and functional characterization of KvLm, a voltage-gated K+ channel from *Listeria monocytogenes*. *J Gen Physiol* 128:283–292.
33. Lundby A, Santos JS, Zazueta C, Montal M (2006) Molecular template for a voltage sensor in a novel K+ channel. II. Conservation of a eukaryotic sensor fold in a prokaryotic K+ channel. *J Gen Physiol* 128:293–300.
34. Braha O, et al. (1997) Designed protein pores as components for biosensors. *Chem Biol* 4:497–505.
35. Mason A (2008) Single-channel characterisation of potassium channels with high temperature studies. DPhil thesis (University of Oxford, Oxford).
36. Rotem D, Mason A, Bayley H (2010) Inactivation of the KcsA potassium channel explored with heterotetramers. *J Gen Physiol* 135:29–42.
37. Tan Q, Shim JW, Gu LQ (2010) Separation of heteromeric potassium channel Kcv towards probing subunit composition-regulated ion permeation and gating. *FEBS Lett* 584:1602–1608.
38. Bayley H, et al. (2008) Droplet interface bilayers. *Mol Biosyst* 4:1191–1208.
39. Holden MA, Needham D, Bayley H (2007) Functional bionetworks from nanoliter water droplets. *J Am Chem Soc* 129:8650–8655.
40. Zheng J, Sigworth FJ (1997) Selectivity changes during activation of mutant Shaker potassium channels. *J Gen Physiol* 110:101–117.
41. Chapman ML, VanDongen AM (2005) K channel subconductance levels result from heteromeric pore conformations. *J Gen Physiol* 126:87–103.
42. Chapman ML, VanDongen HM, VanDongen AM (1997) Activation-dependent subconductance levels in the drk1 K channel suggest a subunit basis for ion permeation and gating. *Biophys J* 72:708–719.
43. Armstrong CM (2003) Voltage-gated K channels. *Sci STKE* 2003:re10.
44. Patlak JB (1999) Cooperating to unlock the voltage-dependent K channel. *J Gen Physiol* 113:385–388.
45. Greenblatt RE, Blatt Y, Montal M (1985) The structure of the voltage-sensitive sodium channel. Inferences derived from computer-aided analysis of the Electrophorus electricus channel primary structure. *FEBS Lett* 193:125–134.
46. Montal M (1990) Molecular anatomy and molecular design of channel proteins. *FASEB J* 4:2623–2635.
47. Patten CD, Caprini M, Planells-Cases R, Montal M (1999) Structural and functional modularity of voltage-gated potassium channels. *FEBS Lett* 463:375–381.
48. Cheley S, et al. (1997) Spontaneous oligomerization of a staphylococcal alpha-hemolysin conformationally constrained by removal of residues that form the transmembrane beta-barrel. *Protein Eng* 10:1433–1443.
49. Montal M, Mueller P (1972) Formation of bimolecular membranes from lipid monolayers and a study of their electrical properties. *Proc Natl Acad Sci USA* 69:3561–3566.
50. Qin F, Auerbach A, Sachs F (1996) Estimating single-channel kinetic parameters from idealized patch-clamp data containing missed events. *Biophys J* 70:264–280.